

## Fabrication and transport characterization of a primary thermometer formed by Coulomb islands in a suspended silicon nanowire

Armin T. Tilke,<sup>a)</sup> Laura Pescini,<sup>b)</sup> Heribert Lorenz, and Robert H. Blick<sup>c)</sup>

Center for NanoScience and Sektion Physik, Ludwig-Maximilians-Universität, Geschwister-Scholl-Platz 1, 80539 München, Germany

(Received 2 January 2003; accepted 27 March 2003)

We realized bolometers in suspended highly *n*-doped silicon nanowires with lateral dimensions down to about 40 nm. Random dopant fluctuations in the suspended wires lead to the formation of multiple tunnel junctions, utilized for Coulomb blockade thermometry. In the low bias regime, we observe relaxation via discrete acoustic phonon modes to give a lower bound for the sensitivity.

© 2003 American Institute of Physics. [DOI: 10.1063/1.1578184]

Bolometric detection of radiation utilizes the temperature increase of a sensor element, e.g., recording detector resistance as a function of incident radiation power. A significant improvement in sensitivity of a thin film bolometer can be obtained by thermally isolating the thermometer from the supporting substrate. This can be achieved either by removing the whole substrate or a sacrificial layer beneath the temperature sensing element.<sup>1</sup> Especially, underetching of thin silicon-on-insulator membranes enables an inexpensive realization of microbolometers.<sup>2</sup>

Electron transport in mesoscopic structures like quantum dots is strongly influenced by Coulomb blockade (CB).<sup>3</sup> CB suppresses tunneling of electrons onto a small conducting island weakly coupled to source and drain leads.<sup>4,5</sup> This argument holds even when a number of quantum dots is placed in a wire forming a set of multitunnel junctions (MTJ), as Pekola *et al.*<sup>6</sup> first showed. Such a MTJ displays CB in the nonlinear  $gV_{DS}$  characteristic, where the conductance  $g$  is defined as  $g = dI_D/dV_{DS}$ ,  $I_D$  being the drain current and  $V_{DS}$  the drain to source voltage. The characteristic shape of the conductance dip in the  $gV_{DS}$  trace turns out to depend only on the electron temperature in the nanostructure and can therefore be utilized as a primary thermometer of unprecedented sensitivity. Although the best system to study CB in tunnel junctions are lithographically defined tunneling barriers,<sup>6,7</sup> dimensions of these structures are usually on the order of several 100 nm. Due to thermal broadening of the Fermi function CB can only be observed as long as the thermal energy  $k_B T$  is smaller than half the charging energy  $E_C$ , that is  $k_B T < e^2/2C = E_C/2$  with  $C$  being the capacitance of the island and  $e$  being the electron charge. Device structures with dimensions of several 100 nm typically exhibit a charging energy of  $E_C \approx 1$  meV corresponding to a temperature of less than 5 K. When  $e^2/C \ll k_B T$  the temperature dependence of the nonlinear  $gV_{DS}$  characteristic in a serial arrangement of tunnel junctions can be approximated according to Ref. 6. The full width at half maximum (FWHM)  $\delta V$  of the nonlin-

ear conductance trace can then be expressed by  $e\delta V \approx N \times 5.44 k_B T$ , for  $N$  identical and homogeneously distributed tunnel junctions in series. This expression is used to determine the local temperature of the tunnel junctions. The exact calculation of the temperature dependence of the nonlinear  $gV_{DS}$  characteristic requires the solution of the corresponding master equation for electron transport through the tunnel junctions. For the case of two tunnel junctions a numerical solution can be derived by using the program TRANS2M by Korotkov.<sup>8</sup>

Recently, Smith *et al.*<sup>9</sup> showed that in highly doped silicon nanowires a serial arrangement of MTJs is formed by random dopant fluctuations, although these tunnel junctions are not identical and their number is not well controlled. The use of nanostructured silicon allows to minimize lateral structure sizes down to about 10 nm.<sup>10</sup> Tighe *et al.* investigated the thermal properties of suspended GaAs nanowires,<sup>11</sup> while Blick *et al.* examined electron transport in suspended GaAs-quantum dots.<sup>12</sup> Fujii *et al.* built suspended *p*-doped silicon nanowires and showed hole transport at room temperature,<sup>13</sup> while Pescini *et al.*<sup>14</sup> first demonstrated electron transport in highly *n*-doped suspended silicon nanowires (SSN) at cryogenic temperatures. Here, we discuss a primary thermometer based on the temperature dependence of a MTJ resonance formed in such highly doped SSN. Moreover, we investigate dissipation at low drain-source bias. Saturation of heat transfer indicates energy relaxation via discrete acoustic phonon modes already around  $T \sim 8$  K.

For the fabrication of the suspended nanowires we use both highly P doped ( $5 \times 10^{19} \text{cm}^{-3}$ ) silicon-on-insulator wafers (SOI) with a silicon film thickness of 170 nm and a 360 nm buried oxide (BOX) and As doped ( $1 \times 10^{20} \text{cm}^{-3}$ ) SOI, with 100 nm Si on 400 nm BOX. First, we define a metallic bow-tie antenna by photolithography and lift-off of 5 nm NiCr and 120 nm Au shown in Fig. 1(b). This antenna is intended to couple the incident radiation to the SSN located in the center of the antenna.<sup>15,16</sup> To fabricate the SSN, we employ low-energy electron beam lithography (acceleration energy 5 keV) with a two-layer poly(methylmethacrylate)-electron resist. Lift-off of a 50-nm-thick Al film creates a hard mask for the subsequent dry etching of the silicon film with  $\text{CF}_4$ . We achieved minimal structure sizes down to about 20 nm.<sup>17</sup> The silicon nano-

<sup>a)</sup>Present address: Infineon Technologies, Königsbrücker Str. 180, 01099 Dresden, Germany.

<sup>b)</sup>Electronic mail: laura.pescini@physik.uni-muenchen.de

<sup>c)</sup>Present address: Electrical and Computer Engineering, University of Wisconsin-Madison, 1415 Engineering Drive, Madison, WI 53706.

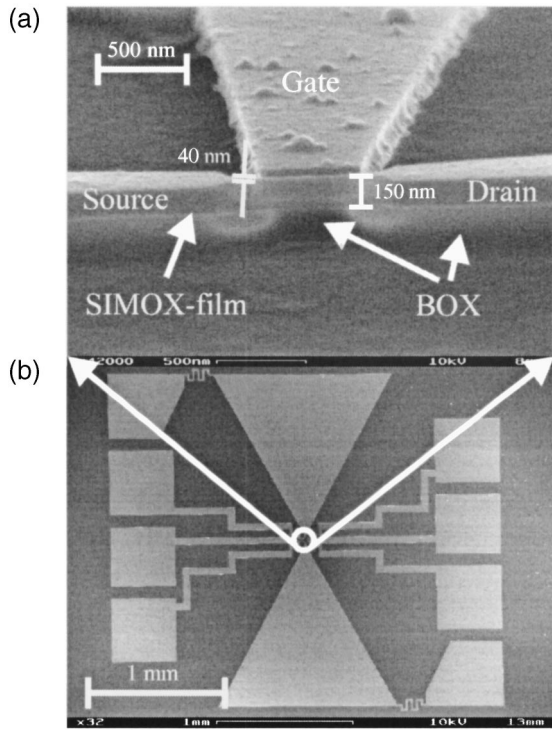


FIG. 1. Suspended nanowire in a sideview (a) demonstrating complete suspension of the wire. The wire is integrated in a bow-tie antenna (b) for achieving maximal radiation coupling.

beams are finally suspended by underetching the BOX in buffered hydro-fluoric acid.<sup>14</sup> Figure 1(a) shows a 40 nm wide, 150 nm thin, and 500 nm long suspended nanowire in a sideview. The devices are then bonded and measured. We used a low-noise current preamplifier and a standard lock-in amplifier operated at a frequency of 130 Hz. Across source and drain a low ac voltage of  $v_{DS}=100 \mu\text{V}$  was applied, whereas for a higher drain-source bias a dc offset  $V_{DS}$  was superimposed to the ac sensing signal.<sup>18</sup>

Figure 2 shows the conductance  $g = dI_D/dV_{DS}$  of the 40 nm wide and 150-nm-thick SSN of Fig. 1 at different tem-

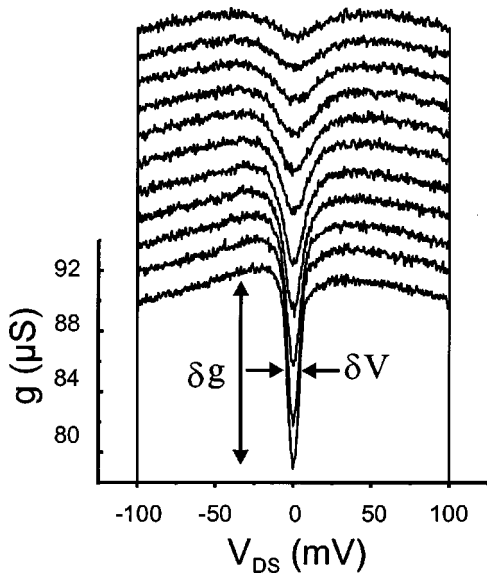


FIG. 2. Temperature dependence of the conductance dip of the suspended nanowire caused by Coulomb blockade. The lowest trace is taken at 1.5 K and the upper most at 16.5 K.

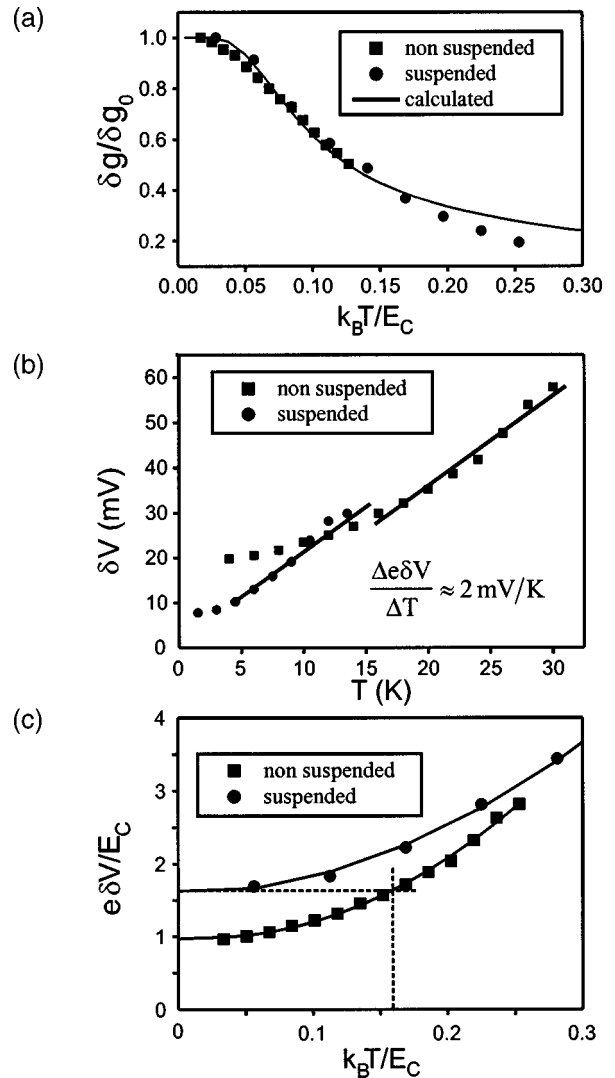


FIG. 3. (a) Temperature dependence of the normalized amplitude of the conductance dip for the suspended and the non suspended wire. Also shown (solid line) is the amplitude calculated by TRANS2M. (b) Temperature dependence of the peak width (FWHM)  $\delta V$  of the conductance dip for the suspended and the nonsuspended wire. The slopes of the curves for high temperatures are almost identical. (c) Normalized  $\delta V$  as a function of temperature normalized to the effective temperature  $T/T_{\text{eff}}=k_B T/E_C$ .

peratures characteristic for MTJs. To understand the peculiarities of electron transport in suspended nanowires, we fabricated nonsuspended wires with a similar degree of  $n$ -doping as for the SSN. The conductance values of all wires are in the same range of  $g \cong e^2/h$ . Since the conductance of the highly doped wires cannot be tuned to zero,<sup>19</sup> in Fig. 3(a) we normalized the height of the conduction dip  $\delta g$  by the extrapolated value at zero temperature  $\delta g_0(T \rightarrow 0)$  and plotted it versus temperature. Also plotted is the curve  $\delta g(T)$  derived by TRANS2M. Introducing an effective temperature  $T_{\text{eff}}=E_C/k_B$  and fitting the  $x$  axis of the experimental data with  $E_C$  as the fit-parameter yields  $E_C=20.5$  meV for the nonsuspended wire and  $E_C=4.62$  meV for the suspended beam. The ratio of  $E_C$  between the two silicon wires is in excellent agreement with the ratio of the wires' cross sections ( $40 \times 150 \text{ nm}^2$  for the suspended and  $45 \times 30 \text{ nm}^2$  for the non suspended wire).

In Fig. 3(b) the temperature dependence of the peak width  $\delta V$  is shown for both wires. The data are approxi-

mated by a linear function with a slope of  $\approx 2$  mV/K also shown in Fig. 3(b). According to Eq. (1) this value indicates a number of  $N \approx 4.3$  tunnel junctions inside the wire. Small deviations from the theoretical expected integer values especially for small  $N$  were also observed in Ref. 7. Most nonsuspended nanowires we measured could be fitted with values of  $N$  ranging from 3 to 5. The nonsuspended wire shown here was chosen so that  $N \approx 4$  in order to be comparable to the suspended beam.

The normalized peak width  $\delta v_{\text{eff}} = e\delta V/E_C$  versus temperature normalized to the effective temperature  $T/T_{\text{eff}}$  is shown in Fig. 3(c). For high  $T/T_{\text{eff}}$  both the suspended as well as the nonsuspended wire show similar behavior with a linear increase of  $\delta v_{\text{eff}}$ . At low temperatures  $k_B T \leq 0.25 E_C$  for both wires  $\delta v_{\text{eff}}$  tends to saturate. For the non suspended wire the extrapolated peak width is  $e\delta V(T \rightarrow 0 \text{ K}) \approx E_C$  as expected from CB theory, whereas the extrapolated peak width for the suspended wire is about a factor of 1.6 higher. At low  $V_{\text{DS}}$  and at low  $T$  the SSN is heated by the electrons passing through, while thermalization is mediated via acoustic phonons. These phonons are radiated into the clamping points acting as reservoirs. Schwab *et al.*<sup>20</sup> and recently Yung *et al.*<sup>21</sup> demonstrated that in suspended semiconductor nanostructures the thermal conductance carried by phonons is quantized, as proposed earlier.<sup>22</sup> Similarly to Refs. 20 and 21 a saturation of the phonon flux towards zero temperature due to phonon quantization can also be expected in our SSN due to the thermal decoupling from the bulk crystal. The effective peak width  $\delta v_{\text{eff}}(T=0 \text{ K}) \approx 1.6$  for the suspended wire corresponds to a temperature of  $T_0 \approx 0.16 E_C/k_B = 8.5 \text{ K}$  [see dashed lines in Fig. 3(c)]. Following Ref. 23 the temperature  $T_q$  from which on mode quantization is observable can be calculated by the wire's cross section. For a wire width of  $w \approx 40 \text{ nm}$  and thickness of  $150 \text{ nm}$  a value of  $T_q \sim 4\text{--}8 \text{ K}$  is obtained being of the same order as  $T_0$ . The variation is related to different sound velocities of acoustic phonons in the bulk and at the surface. The deviation from  $\delta v_{\text{eff}}(T=0 \text{ K}) = 1$  for the suspended wire is therefore caused by a temperature saturation, whose limit is given by phonon quantization as outlined in Ref. 24. For the application of the SSN this indicates a lower bound for sensitivity at low temperatures.

At temperatures  $T \gg T_0$  dissipation in the SSN due to ohmic losses can be approximated in first order by uniform heating of the wire with length  $l$ , thickness  $d$ , and width  $w$ . The thermal conductance  $G$  of the wire can then be calculated using  $G = 12\kappa w d/l$ , with  $\kappa$  the thermal conductivity.<sup>2</sup> In suspended bolometers with dimensions of some  $10 \mu\text{m}$ ,  $G$  can be found to be about  $2 \times 10^{-5} \text{ W/K}$ .<sup>2</sup> Calculating  $G$  for an SSN with dimensions of  $d = 150 \text{ nm}$ ,  $l = 500 \text{ nm}$ , and  $w = 40 \text{ nm}$  and using  $\kappa \leq 2000 \text{ W/(m K)}$ <sup>25</sup> for bulk silicon we find values of  $\sim 3 \times 10^{-4} \text{ W/K}$  at temperatures  $T \geq 10 \text{ K}$ . The time constant  $\tau$  for resistive heating of the wire is given by

$$\tau = \frac{C_T}{G} = \frac{\rho c l^2}{12\kappa}, \quad (1)$$

with the thermal capacitance  $C_T$ , the density of silicon  $\rho \approx 2.3 \times 10^3 \text{ kg/m}^3$  and the specific heat  $c \approx 0.3 \text{ J/(kg K)}$ . At

$T \approx 10 \text{ K}$ ,  $\tau$  is expected to be on the order of only  $10^{-14} \text{ s}$ . This very small time constant would allow the very fast operation of a bolometer comprising such an SSN. Additionally, a small  $\tau$  leads to a very high sensitivity of the bolometer. Moreover, the thermal conductance of bulk silicon with an  $n$ -doping concentration of  $1 \times 10^{20} \text{ cm}^{-3}$  around  $3 \text{ K}$  is about  $3 \text{ W/m}^{-1} \text{ K}^{-1}$ . This is two orders of magnitude below that of pure silicon,<sup>26</sup> which reduces  $\tau$  even further.

In summary we realized suspended highly  $n$ -doped silicon nanowires that display Coulomb blockade behavior at temperatures up to  $20 \text{ K}$  due to the formation of multiple tunnel junctions. These MTJs can be used as a primary thermometer sensing the local temperature of the suspended wire. The setup can therefore be utilized as an ultrasensitive bolometer.

The authors would like to thank A. Erbe, F. C. Simmel, J. P. Kotthaus, and M. L. Roukes for detailed discussions and A. Kriele and S. Manus for technical support. The authors acknowledge financial support from the Bundesministerium für Forschung und Technologie (BMBF-01BM914) and the Deutsche Forschungsgemeinschaft (DFG-QIV: BI-487/2).

- <sup>1</sup>H. Neff, J. Laukemper, I. A. Krebtov, A. D. Tkachenko, E. Steinbeiss, W. Michalke, M. Burnus, T. Heidenblut, G. Hefle, and B. Schwierzi, *Appl. Phys. Lett.* **66**, 2421 (1995).
- <sup>2</sup>L. Mechin and J.-C. Villegier, *Appl. Phys. Lett.* **70**, 123 (1997).
- <sup>3</sup>T. A. Fulton and G. J. Dolan, *Phys. Rev. Lett.* **59**, 109 (1987).
- <sup>4</sup>C. W. J. Beenakker, *Phys. Rev. B* **44**, 1646 (1991).
- <sup>5</sup>H. van Houten, C. W. J. Beenakker, and A. A. M. Staring, in *Single Charge Tunneling*, edited by H. Grabert and M. H. Devoret (Plenum, New York, 1992), p. 167.
- <sup>6</sup>J. P. Pekola, K. P. Hirvi, J. P. Kauppinen, and M. A. Paalanen, *Phys. Rev. Lett.* **73**, 2903 (1994).
- <sup>7</sup>K. P. Hirvi, J. P. Kauppinen, A. N. Korotkov, M. A. Paalanen, and J. P. Pekola, *Appl. Phys. Lett.* **67**, 2096 (1995).
- <sup>8</sup>A. Korotkov, FORTRAN program TRANS2M, 1991.
- <sup>9</sup>R. A. Smith and H. Ahmed, *J. Appl. Phys.* **81**, 2699 (1997).
- <sup>10</sup>A. Tilke, R. H. Blick, H. Lorenz, and J. P. Kotthaus, *J. Appl. Phys.* **89**, 8159 (2001).
- <sup>11</sup>T. S. Tighe, J. M. Worlock, and M. L. Roukes, *Appl. Phys. Lett.* **70**, 2687 (1997).
- <sup>12</sup>R. H. Blick, F. G. Monzon, W. Wegscheider, M. Bichler, F. Stern, and M. L. Roukes, *Phys. Rev. B* **62**, 17103 (2000).
- <sup>13</sup>H. Fujii, S. Kanemaru, T. Matsukawa, and J. Itoh, *Appl. Phys. Lett.* **75**, 3986 (1999).
- <sup>14</sup>L. Pescini, A. Tilke, R. H. Blick, H. Lorenz, J. P. Kotthaus, W. Eberhardt, and D. Kern, *Nanotechnology* **10**, 418 (1999).
- <sup>15</sup>N. Chong and H. Ahmed, *Appl. Phys. Lett.* **71**, 1607 (1997).
- <sup>16</sup>D. P. Osterman, R. Patt, R. Hunt, and J. B. Peterson, *Appl. Phys. Lett.* **71**, 2361 (1997).
- <sup>17</sup>A. Tilke, L. Pescini, H. Lorenz, and R. H. Blick, *Nanotechnology* **13**, 491 (2002).
- <sup>18</sup>A. T. Tilke, F. C. Simmel, R. H. Blick, H. Lorenz, and J. P. Kotthaus, *Prog. Quantum Electron.* **25/3**, 97 (2001).
- <sup>19</sup>A. Tilke, R. H. Blick, H. Lorenz, D. A. Wharam, and J. P. Kotthaus, *Appl. Phys. Lett.* **75**, 3704 (1999).
- <sup>20</sup>K. Schwab, E. A. Henriksen, J. M. Worlock, and M. L. Roukes, *Nature (London)* **404**, 974 (2000).
- <sup>21</sup>C. S. Yung, D. R. Schmidt, and A. N. Cleland, *Appl. Phys. Lett.* **81**, 31 (2002).
- <sup>22</sup>L. G. C. Rego and G. Kirczenow, *Phys. Rev. Lett.* **81**, 232 (1998); M. A. Stroschio, Y. M. Sirenko, S. Yu, and K. W. Kim, *J. Phys. C* **8**, 2143 (1996).
- <sup>23</sup>K. Johnson, M. N. Wybourne, and N. Perrin, *Phys. Rev. B* **50**, 2035 (1994).
- <sup>24</sup>B. A. Glavin, *Phys. Rev. Lett.* **86**, 4318 (2001).
- <sup>25</sup>*Properties of SILICON*, EMIS Datareviews Series No. 4 (INSPEC, London, 1988).
- <sup>26</sup>G. A. Slack, *J. Appl. Phys.* **35**, 3460 (1964).